# Bilayer-Barrier Ferroelectric-$HfO_2$ Tunnel Junction with High ON Current and Giant ON/OFF ratio Arising from Resonant Tunneling

Pengying Chang*, Yirong Guo, Jie Li, Yiyang Xie*
*Key Laboratory of Optoelectronics Technology, Ministry of Education, Beijing University of Technology, Beijing, China*
pychang@bjut.edu.cn; xieyiyang@bjut.edu.cn

***Abstract*—The hafnium oxide ($HfO_2$) based ferroelectric tunnel junction (FTJ) using ferroelectric-dielectric (FE-DE) bilayer-barrier structure is studied by physical modeling. The FTJ performance strongly depends on the barrier height of DE with respect to that of FE-$HfO_2$. Compared with FE-$HfO_2$/$SiO_2$ case, FE-$HfO_2$/$Ta_2O_5$ based FTJ shows high ON current ($J_{ON}$) and giant ON/OFF ratio. The underlying physics is to introduce resonant tunneling (RT) by forming a quantum well and to shift resonance peak close to the Fermi level. The switching between the direct tunneling (DT) and RT under different polarization direction leads to an enhanced TER effect.**

***Keywords—Ferroelectric tunnel junction, resonant tunneling, tunneling electroresistance, hafnium oxide***

## I. Introduction

Ferroelectric tunnel junctions (FTJ) have attracted great attention as novel nonvolatile memory devices [1], especially due to the discovery of the CMOS-compatible ferroelectric (FE) hafnium oxide ($HfO_2$) [2]. The basic working principle of the ON/OFF tunneling electroresistance (TER) in FTJ is controlled by ferroelectric polarization switched by electric field. The carrier transport across the nanometer-thick FE film is governed by quantum-mechanical tunneling [3]. Up to now, the FE-$HfO_2$ based FTJs including MFM, MFS, MFIM and MFIS structures are mainly based on the directing (DT) or Fowler-Nordheim (FN) tunneling mechanisms [4],[5],[6]. However, these single-barrier or bilayer-barrier FE-$HfO_2$ FTJs inevitably suffer from the compromise between the ON-current ($J_{ON}$) and ON/OFF ratio (i.e. TER ratio). Even using the asymmetrical FE-DE (such as $SiO_2$ or $Al_2O_3$ DEs) bilayer barrier, it is still hard to satisfy the requirements of $J_{ON}$ and ON/OFF ratio for large array application[7]. Besides the DT and FN, another mechanism that is not explored enough is the resonant tunneling (RT) [8]. We have recently proposed asymmetric barrier-well-barrier (three-layer) based resonant FTJ, where a low-barrier DE such as $Ta_2O_5$ is inserted between two barriers to introduce the RT [9],[10]. In this work, we propose that the bilayer-barrier FTJ with sufficient thick low-barrier DE are also able to form a quantum well under only one polarization direction, which achieves a switch between DT and RT under reversed polarization direction and leads to an enhanced TER effect.

## II. Simulation Method

Fig. 1 shows schematics of bilayer FE-$HfO_2$ FTJ devices using high-barrier $SiO_2$ and low-barrier $Ta_2O_5$ as interfacial dielectric. Symmetric top (TE) and bottom electrode (BE) is assumed using TiN, as we focuses on the FE-DE bilayer-barrier engineering. Fig. 2 shows the simulation framework that consists of two parts. The first part is self-consistent potential calculation. The bias voltage $V_a$ drops across the TE and BE ($V_{m1}$ and $V_{m2}$), interfacial dielectric ($V_{IL}$), and ferroelectric ($V_{FE}$). The metal screening effect is considered by Thomas-Fermi model. The FE polarization is descripted by Preisach model. The second part is current density calculation. The transmission coefficient (TC) is obtained by transfer matrix method (TMM) to get resonant tunneling. The supply function N of electrons is obtained based on Fermi-Dirac distribution. Then current density J is calculated by Tsu-Esaki formula based on the integral of TC multiplying N (TC×N) versus electron energy E. The FE thickness $T_{FE}$ is set as 4 nm, and permittivity of FE-$HfO_2$, $SiO_2$ and $Ta_2O_5$ are set as 25, 3.9 and 25 respectively. The screening lengths of TiN are set as 0.5 Å. All the remaining parameters used in the simulation are consistent with [9],[10]. Physical model calibration with experimental I-V curves of FTJs is shown in [9].

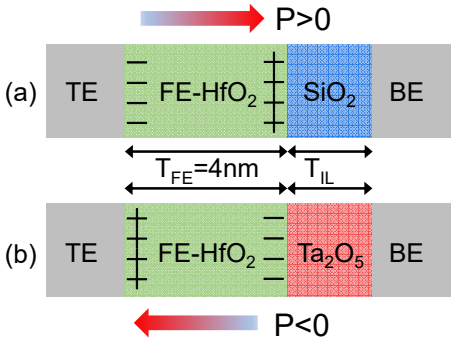


Fig. 1 Schematics of FE-DE bilayer FE-$HfO_2$ FTJ devices using (a) high-barrier $SiO_2$ and (b) low-barrier $Ta_2O_5$ as interfacial dielectric. Symmetric top and bottom electrode is assumed using TiN.

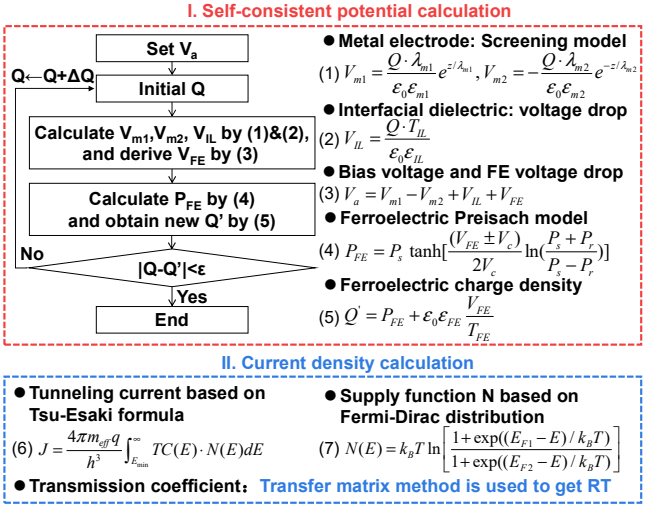


Fig. 2 Simulation framework consists of two parts: self-consistent calculation of electrostatic potential and current density calculation.

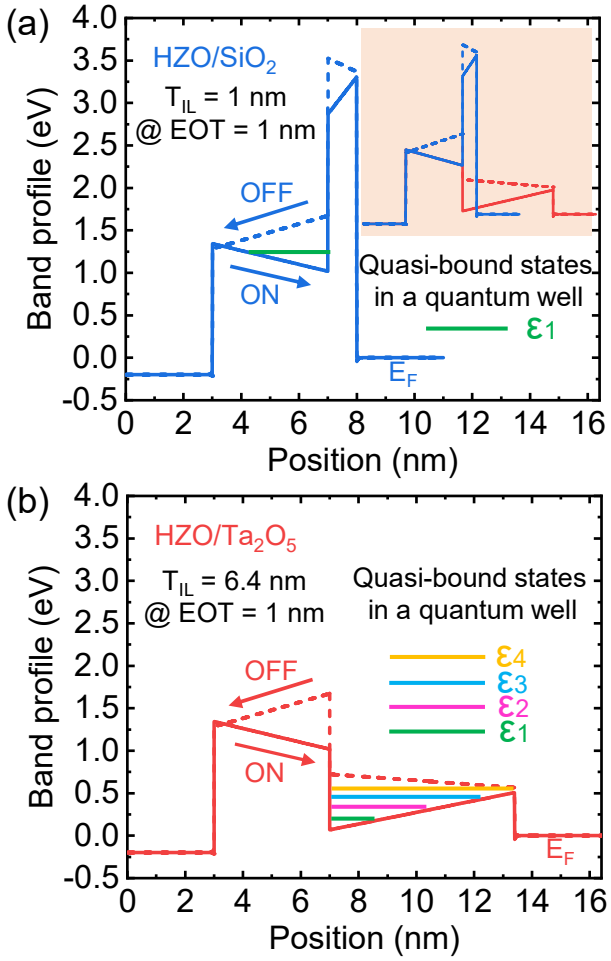


Fig. 3 Band diagrams of (a) $HZO/SiO_2$ and (b) $HZO/Ta_2O_5$ based FTJ with read voltage of 0.2V under ON and OFF states. A quantum well with confined states is formed only at ON state. The EOT of interfacial layer is set as 1 nm (i.e., $T_{IL}$ is 1nm for $SiO_2$, and 6.4nm for $Ta_2O_5$), so that the FE films are affected by the exactly identical $E_{dep}$, as shown by the totally overlapped band diagrams cross FE film in the insert of (a).

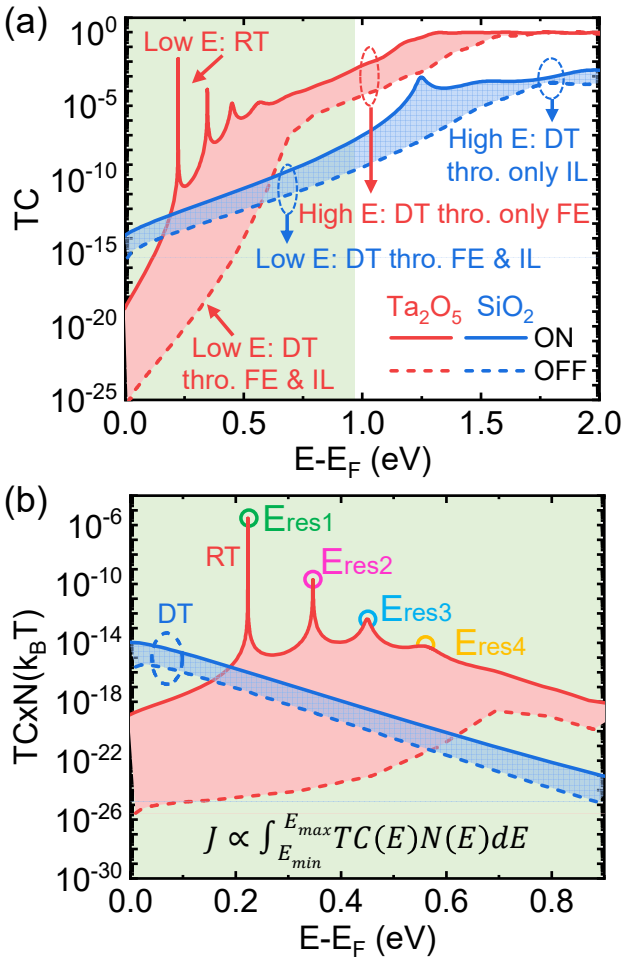


Fig. 4 (a) Related TC-E curves, where carrier transport by DT and RT is labeled. The electron tunneling with energy exceeding a certain range (~0.95 eV at 300 K) is negligible with the assumption of Fermi-Dirac distribution. (b) Related TC×N-E curves within 0.95 eV, where the resonance energy levels $E_{resn}$ correspond to quantized energy levels $\varepsilon_n$ as shown in Fig. 3.

## III. Results and Discussion

### A. Carrier Transport Properties

Fig. 3(a) and (b) show the band diagrams of $HZO/SiO_2$ and $HZO/Ta_2O_5$ based FTJ with read voltage of 0.2V under ON and OFF states. In both cases, the average barrier height is lowered (raised) at ON (OFF) state, when FE polarization points towards the BE (TE). At ON state, a quantum well (QW) with confined states is formed at the lower one of bilayer barrier. That is to say, the QW is located in the FE layer in $HZO/SiO_2$ stack, whereas it is in the DE layer in $HZO/Ta_2O_5$ stack. To fairly considering the effect of DE barrier engineering, the EOT of interfacial DE layer is set as 1 nm (i.e., $T_{IL}$ is 1nm for $SiO_2$, and 6.4nm for $Ta_2O_5$ respectively), so that the FE films are affected by the exactly identical depolarization field $E_{dep}$, as shown by the totally overlapped band diagrams cross FE film in the insert of (a). Moreover, there is only one quasi-bound state in $HZO/SiO_2$ stack, and the corresponding confined energy $\varepsilon_1$ is far away from the Fermi energy $E_F$ at the cathode. In contrast, there are four quasi-bound states in $HZO/Ta_2O_5$ stack, and the corresponding confined energies are much closer to the $E_F$ due to the low barrier height of $Ta_2O_5$. Therefore, the QW in bilayer stack can be appropriately modulated by engineering the DE layer though film thickness and barrier shape.

Fig. 4(a) shows the related TC-E curves, where carrier transport by DT and RT is labeled depending on the polarization direction and electron energy. For $HZO/SiO_2$ stack, the carrier transport is almost dominated by the DT process. The carriers with low E tunnel across both HZO and $SiO_2$ layers. As E increases, carrier tunnel across $SiO_2$ only. Note that there is a weak TC resonance peak around 1.25 eV at ON state arising from the shallow QW as shown in Fig. 3(a). For $HZO/Ta_2O_5$ stack, the carrier transport with high E is dominated by DT across the HZO layer at both ON and OFF states. However, when E is low, there is a switching between the DT and RT depending on the polarization direction. At OFF state, carrier transport is dominated by DT across both HZO and $Ta_2O_5$ layers. In contrast, at ON state, carrier transport is dominated by RT. Particularly, the resonance peaks in $HZO/Ta_2O_5$ case are sharper and are located lower in energy, compared with $HZO/SiO_2$ case.

Fig. 4(b) show the related TC×N-E curves that determine the current density, where the resonance energy levels $E_{resn}$ correspond to quantized energy levels $\varepsilon_n$. Note that the electron tunneling with energy exceeding a certain range

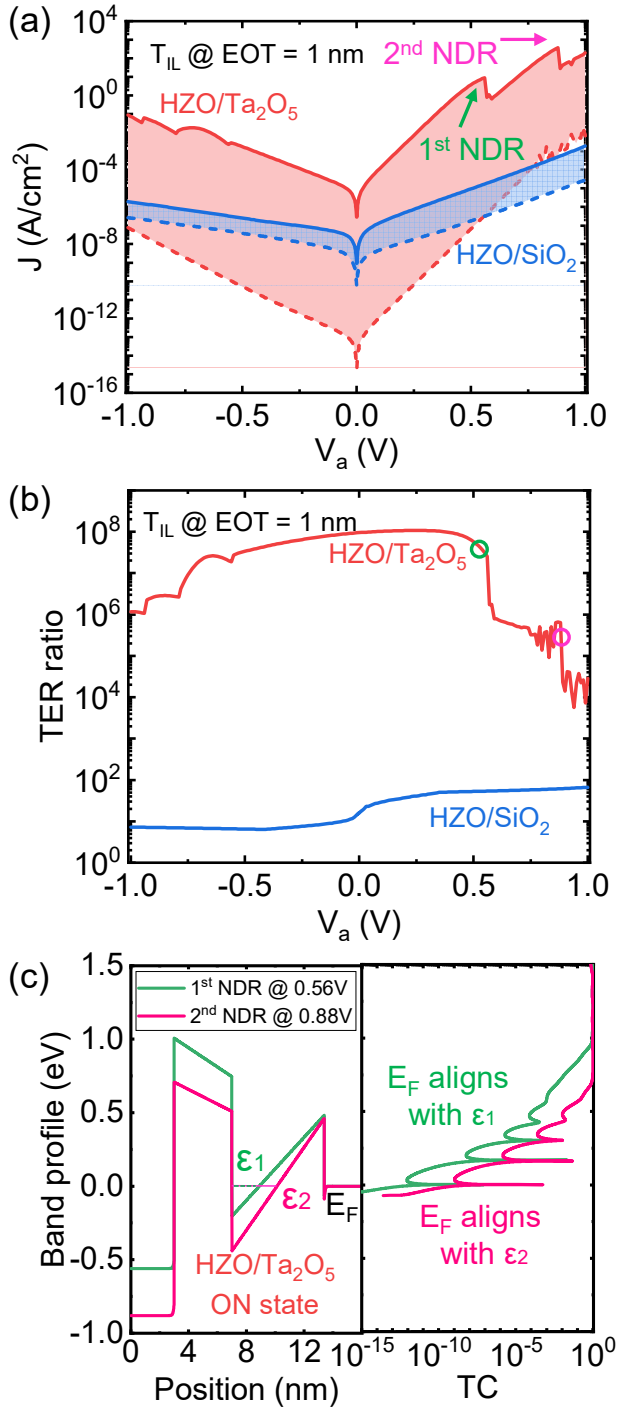


Fig. 5 (a) Current density and (b) TER ratio versus $V_a$ in two FTJs with IL EOT of 1nm. (c) Band profiles and related TC curves for ON-state HZO/$Ta_2O_5$ based FTJ at $V_a$ of 0.56 V and 0.88 V respectively.

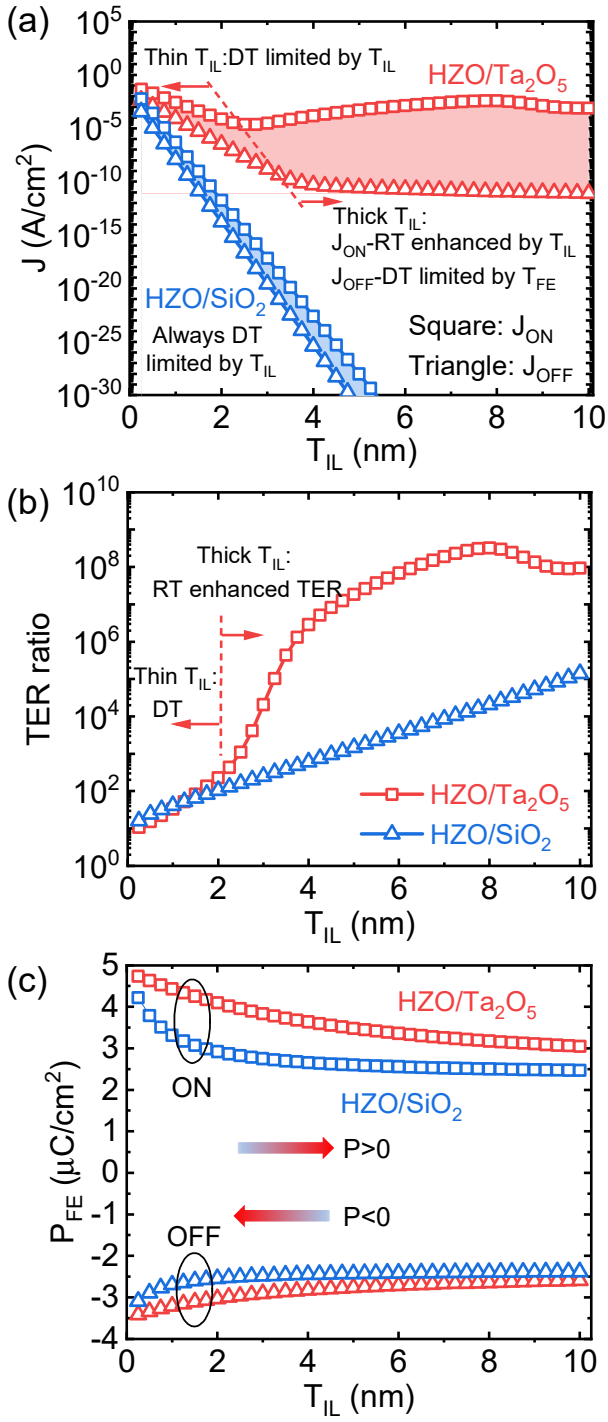


Fig. 6 (a) Current density, (b) TER ratio, and (c) $P_{FE}$ as a function of interfacial DE thickness $T_{IL}$ at 0.2V.

[~0.95 eV at 300 K based on carrier supply function N in (7) in Fig. 2] is negligible because the high-energy tail is limited due to Fermi-Dirac distribution. Therefore, TC×N-E curves are plotted for E below 0.95 eV. Moreover, supply function N decays exponentially with E. When $E_{res}$ is close to $E_F$, resonance-induced tunneling current will be larger due to a larger number of carriers being supplied close to $E_F$. From Fig. 4(b), it is expected that the $J_{ON}$ and TER ratio in FTJs can be significantly improved using HZO/$Ta_2O_5$ stack compared with HZO/$SiO_2$ stack, which will be revealed in the following.

### *B. Performance Comparison*

Fig. 5(a) and (b) shows the current density and TER ratio versus $V_a$ in two FTJs with EOT of 1 nm. Compared with HZO/$SiO_2$, $J_{ON}$ in HZO/$Ta_2O_5$ based FTJ is greatly improved benefiting from low barrier height and resonant tunneling, whereas $J_{OFF}$ is markedly reduced due to the thick DE layer suppressing the DT. Consequently, TER ratio of HZO/$Ta_2O_5$ based FTJ is improved by several orders of magnitude. Besides, the negative differential resistance (NDR) effects take place when the $E_F$ in the cathode aligns with $\varepsilon_n$, beyond which $J_{ON}$ and TER ratio then suddenly drops. As shown in

Fig. 5(c), the first NDR takes place at 0.56 V, when $E_F$ aligns with first confined-state energy level $\mathcal{E}_1$ in the QW. The second NDR takes place at 0.88 V, when $E_F$ aligns with second confined-state energy level $\mathcal{E}_2$ in the QW.

Fig. 6 shows the current density, TER ratio, and ferroelectric polarization $P_{FE}$ as a function of $T_{IL}$ at 0.2V respectively. For HZO/$SiO_2$, both $J_{ON}$ and $J_{OFF}$ is dominated by DT, which are very sensitive to $T_{IL}$ due to high barrier of $SiO_2$. For HZO/$Ta_2O_5$, two distinct conduction regions are observed depending on $T_{IL}$ as divided by dash line in Fig. 6(a). When $T_{IL}$ is thin, current and carrier behave similarly to that of HZO/$SiO_2$. When $T_{IL}$ is thick, $J_{ON}$ is dominated by RT because resonance peaks are located close to $E_F$. However, $J_{OFF}$ is still dominated by DT, but is limited by $T_{FE}$ and almost independent on $T_{IL}$. The reason is that carriers with energy of 0.6~0.9 V that tunnel through FE film only contribute most to the current as seen in Fig. 4(b), while carriers with energy below 0.6 eV that tunnel through both FE and DE film is almost totally suppressed due to the wide tunneling thickness. Moreover, $P_{FE}$ in HZO/$Ta_2O_5$ is slightly larger, meaning that $E_{dep}$ is smaller benefiting from high permittivity of $Ta_2O_5$.

## IV. Conclusion

Device performance of bilayer-barrier FE-$HfO_2$ FTJ can be engineered by selecting different interfacial dielectrics, depending on the tunneling barrier height, barrier thickness and barrier shape. The HZO/$SiO_2$ FTJ suffers from a serious tradeoff between $J_{ON}$ and TER ratio, because high-barrier $SiO_2$ leads to reduced current density. In contrast, HZO/$Ta_2O_5$ FJT shows simultaneous improvement of $J_{ON}$ and TER ratio, originating from the resonant tunneling induced by thick and low-barrier $Ta_2O_5$ quantum well. The switching between the direct tunneling and resonant tunneling under reversed polarization direction leads to an enhanced TER effect, making resonant FTJ suitable for large array circuits.


## Acknowledgment

This work was supported in part by the Beijing Natural Science Foundation under Grant 4232061, in part by the BPHR202203024, and in part by the National Natural Science Foundation of China under Grant 61804003.


## References


[1] X. Wang and J. Wang, "Ferroelectric tunnel junctions with high tunneling electroresistance," *Nat. Electron.*, vol. 3, pp. 440-441, Aug. 2020.

[2] P. Chang, Y. Zhang, G. Du, and X. Liu, "Experiment and Modeling of Dynamical Hysteresis in Thin Film Ferroelectrics," *Jpn. J. Appl. Phys.*, vol. 59, pp. SGGA07, Feb.2020.

[3] M. Y. Zhuravlev, R. F. Sabirianov, S. S. Jaswal, and E. Y. Tsymbal, "Giant electroresistance in ferroelectric tunnel junctions," *Phys. Rev. Lett.*, vol. 94, no. 24, pp. 246802, Jun. 2005.

[4] Z. Wen, C. Li, D. Wu, A. Li, and N. Ming, "Ferroelectric-field-effect enhanced electroresistance in metal/ferroelectric/semiconductor tunnel junctions," *Nature Mater.*, vol. 12, no. 7, pp. 617-621, Jul. 2013

[5] P. Chang, G. Du, J. Kang, and X. Liu, "Conduction Mechanisms of Metal-Ferroelectric-Insulator-Semiconductor Tunnel Junction on N- and P-Type Semiconductor," *IEEE Electron Device Lett.*, vol. 42, no. 1, pp. 119-121, Jan. 2021.

[6] P. Chang, G. Du, J. Kang, and X. Liu, "Guidelines for Ferroelectric-Semiconductor Tunnel Junction Optimization by Band Structure Engineering," *IEEE Trans. Electron Devices*, vol. 68, no. 7, pp. 3526-3531, May 2021.

[7] Y.-C. Luo, J. Hur, and S. Yu, "Ferroelectric tunnel junction based crossbar array design for neuro-inspired computing," *IEEE Trans. Nanotechnol.*, vol. 20, pp. 243-247, Mar. 2021.

[8] Y. Ando and T. Itoh, "Calculation of transmission tunneling current across arbitrary potential barriers," *J. Appl. Phys.*, vol. 61, no. 4, pp. 1497-1502, Feb. 1987.

[9] P. Chang, and Y. Xie, "Evaluation of $HfO_2$-Based Ferroelectric Resonant Tunnel Junction by Band Engineering," *IEEE Electron Device Lett.*, vol. 44, no. 1, pp. 168-171, Jan. 2023.

[10] P. Chang, and Y. Xie, "Ferroelectric Tunnel Junction Based on Asymmetric Barrier-Well-Barrier Structure: The Role of Resonant Tunneling," *IEEE Trans. Electron Devices*, vol. 70, no. 5, pp. 2282-2290, May. 2023.